Transactions, SMiRT-24
BEXCO, Busan, Korea - August 20-25, 2017
Division 03

INTERACTION OF BENDING AND PUNCHING OF REINFORCED CONCRETE SLABS SUBJECTED TO IMPACT BY DEFORMABLE MISSILES IN IMPACT III PROJECT TESTS

Michael Borgerhoff[1], Claudia van Exel[1], Javier Rodríguez[2], Luis Lacoma[2], Christian Schneeberger[3], Friedhelm Stangenberg[1], and Rainer Zinn[1]

[1] Stangenberg und Partner Ingenieur-GmbH (SPI), Consulting Engineers, Bochum, Germany (borgerhoff@stangenberg.de)
[2] Principia Ingenieros Consultores S.A., Madrid, Spain
[3] Swiss Federal Nuclear Safety Inspectorate ENSI, Brugg, Switzerland

ABSTRACT

Phase III of the IMPACT project includes a series of experiments with reinforced concrete slabs subjected to impact by deformable missiles, which have the objective of investigating the combined effect of longitudinal and transverse reinforcement in the range of ultimate load capacity. More specifically, the structural design of the slabs and the actions by the impacting missiles aim at achieving the plastic capacity both in bending and shear. Subject to these conditions, the influence of different combinations of longitudinal and transverse reinforcement in terms of amount and constructive design is examined.

The test specimens of the combined bending and punching tests are reinforced concrete slabs with dimensions 2.1 m x 2.1 m x 0.25 m. As impacting missiles, steel pipes with a uniform weight of 50 kg but different wall thicknesses and impact velocities up to 168 m/s have been used. The IMPACT project is organised and carried out by VTT in Espoo (Finland) and funded by several institutions including ENSI.

In the last two SMiRT conferences, the authors have reported on conclusions gained from the first four combined bending and punching tests. The further tests recently carried out are subject of the evaluation and assessment in this paper, while the results are related to the findings of the first tests. The experiments are numerically simulated by nonlinear dynamic analyses using different FE programs for different types of models. The outcomes are used to improve the capabilities of shell element models for simulation of punching problems. Another focus is on the accuracy of empirical formulae for the prediction of perforation loads under soft missile impact.

INTRODUCTION

The investigation results presented in this paper emerged from the continuation of the collaborative effort between the Swiss Federal Nuclear Safety Inspectorate (ENSI) and their consultants Principia and SPI. ENSI participates in the IMPACT III project organised by the VTT Technical Research Centre of Finland and funded by several institutions including ENSI, see also Borgerhoff et al. (2013, 2015) and Zinn et al. (2014). The aim of this project is to develop experimental data and information on physical phenomena occurring during an aircraft impact on a reinforced concrete (r/c) structure. The specific issue of the tests presented in this paper is to examine the influence of different types of transverse reinforcement (tests X5 to X8), and the influence of changing ratios of longitudinal and transverse reinforcement (tests X9, X10) on the interaction of bending and punching, while the effects produced by the impact are very close to the ultimate load capacity of the slab in bending as well as shear.

EXECUTION OF TESTS X5 TO X10

The experiments for tests X5 to X10 on r/c panels with the outer dimensions 2.087 m x 2.087 m x 0.25 m (spans 2.0 m) were carried out by VTT in 2016 (X5 to X8) and 2017 (X9, X10). The test data used for the numerical simulation are summarised in Table 1. In order to achieve a broad comparability of the test results, the test slabs of each series (X5 to X8, and X9, X10) were produced from the same concrete type and were concreted on the same day, respectively. Minor differences in the respective concrete strengths result from the fact that not all tests could be carried out on the same day.

Test X5 without transverse reinforcement was carried out with the objective of obtaining more accurate knowledge of the concrete proportion of the punching capacity upon impact of a deformable projectile. The plastic deformation resistance of the projectile dependent on the tube wall thickness and the impact velocity were determined correctly on the basis of empirical formulas, so that in the experiment the intended formation of a punching cone with activation of the dowel effect of the bending reinforcement was achieved without a perforation of the slab. The objective of the three tests X6 to X8 was to investigate the influence of different types of shear reinforcement on the punching capacity. The selection of the shear reinforcement cross-section 34.9 cm²/m² has ensured that the load-bearing capacity was almost reached in all three tests, see Figure 1. The types of shear reinforcement were closed stirrups (X6), T-headed bars (X7), and C-shaped stirrups (X8). The objective of the two further tests X9 and X10 was to assess the effect of different bending reinforcement ratios on the interaction of bending and punching behaviour, which was realised by changing the bar diameter of the longitudinal reinforcement.

Table 1: IMPACT III, dates of tests X5 to X8 (carried out in 2016), and X9, X10 (carried out in 2017).

Test		X5	X6	X7	X8	X9	X10
Slab thickness	[m]	0.25					
Slab dimensions	[m]	2.087 x 2.087					
Span width	[m]	2.0 x 2.0					
Bending reinforcement	[cm²/m]	Ø 10 mm, c/c 90 mm, e.s.e.w. → 8.7				Ø 8 mm, c/c 90 mm, e.s.e.w. → 5.6	Ø 12 mm, c/c 90 mm, e.s.e.w. → 12.6
Shape of shear reinforcement		—	Closed stirrups	T-headed bars	Hooked stirrups		
Shear reinforcement	[cm²/m²]	—	Ø 8 mm, c/c 90 mm / 160 mm → 34.9				
Date of concreting		01.02.2016				03.01.2017	
Date of test		18.3.2016	03.03.2016	09.03.2016	15.03.2016	14.03.2017	07.03.2017
Concrete age	[d]	46	31	37	43	70	63
Compressive strength	[MPa]	≈ 59	≈ 55	≈ 57	≈ 58	≈ 62	≈ 61
Tensile strength	[MPa]	≈ 3.6	≈ 3.0	≈ 3.2	≈ 3.5	≈ 3.1	≈ 3.1
Impact velocity	[m/s]	162.5	166.7	166.5	166.7	165.1	165.7
Projectile wall thickness	[mm]	3.0	6.35				
Projectile mass	[kg]	50					

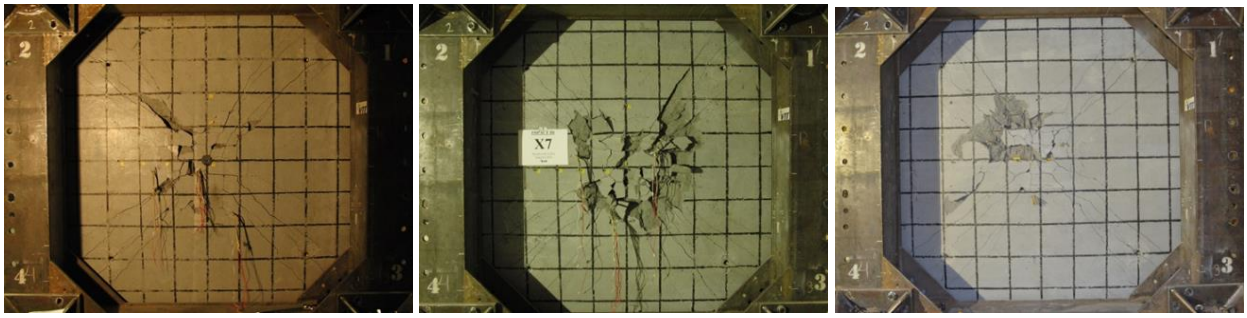

Figure 1. Crack formation on the reverse side of the slabs in tests X6 to X8 (from left to right).

NUMERICAL SIMULATION OF TEST X5

For test X5, Principia performed computational analyses with the coupled finite element (FE) model shown in Figure 2 by use of the Abaqus program, SIMULIA (2013). The model consists of volume elements (concrete slab), beam elements (bending reinforcement) and shell elements (projectile). In the Figures 3 and 4, the plastic concrete compressive strains of the deformed model structure and the strains of the bending reinforcement in the horizontal symmetry axis are shown in form of time histories. Figure 3 also shows a horizontal section through the concrete slab sawn off after the test, showing a clear punching without complete perforation of the slab in the hit area. The results of the calculations carried out thus confirm the test result. The magnitude of the measured strains of the bending reinforcement shown in Figure 4 is matched fairly well by the results of the Abaqus calculation.

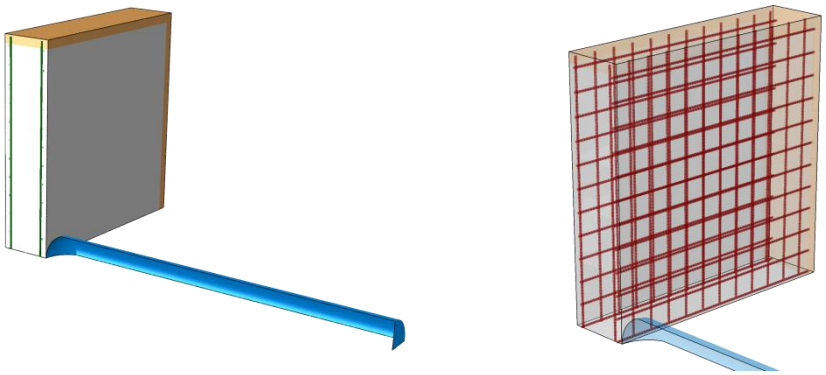

Figure 2. Test X5, coupled Abaqus FE model and reinforcement mesh.

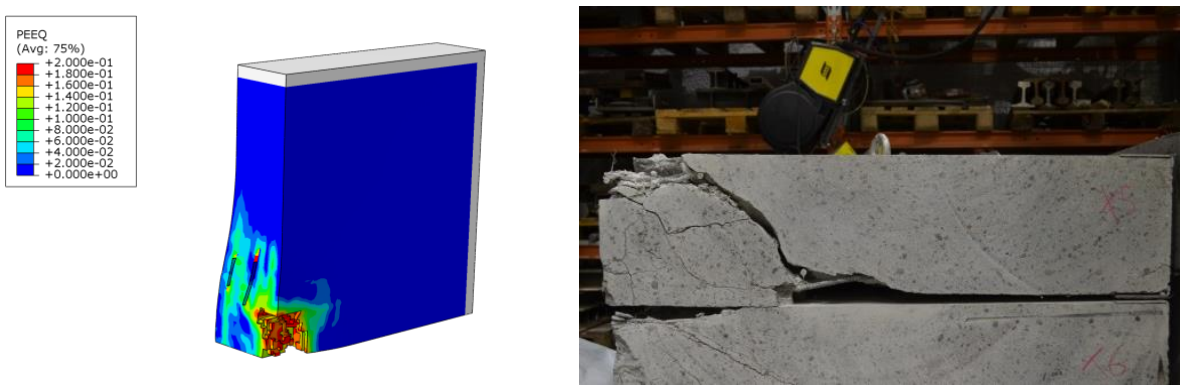

Figure 3. Test X5, calculated plastic concrete compressive strains compared to a horizontal section through the test slab with punching cone.

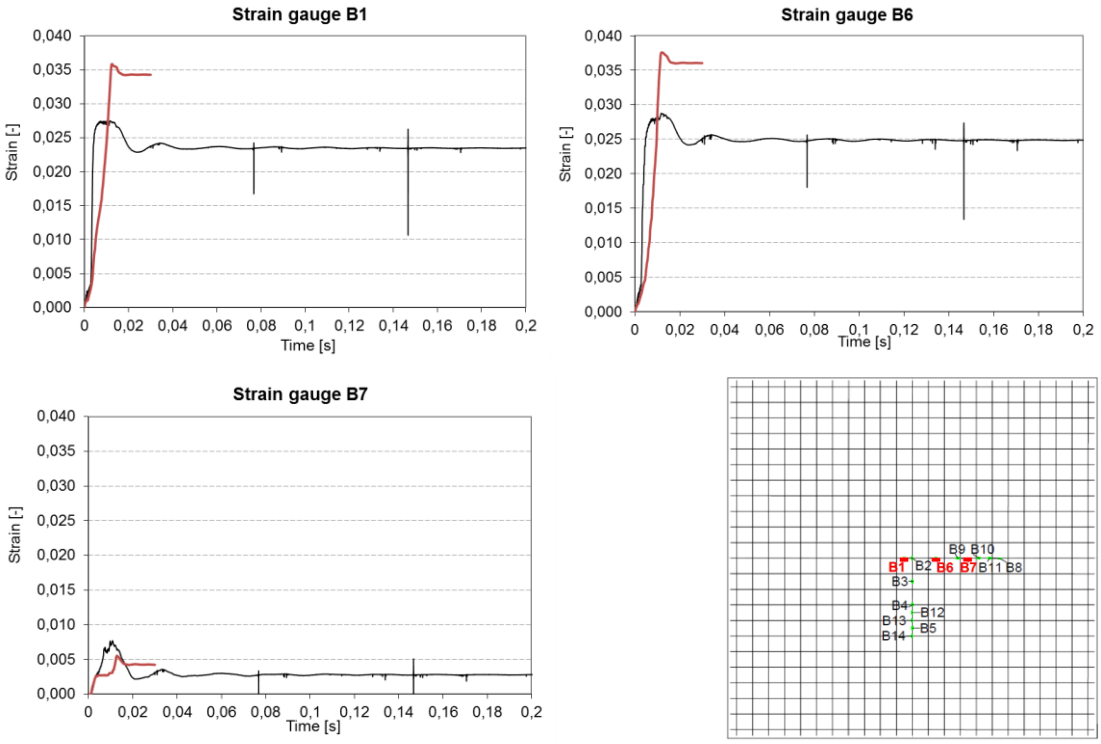

Figure 4: Test X5, calculated (red curves) and measured (black curves) strains of bending reinforcement in the horizontal symmetry axis.

The contribution of concrete as part of the punching shear capacity, which is equivalent to the full capacity in test X5 having no shear reinforcement, according to German standard DIN 25449, is 0.86 MN. The average load of 0.68 MN derived from the diagram of Figure 5 does not exceed the punching shear capacity, hence a perforation was not expected in test X5. As visible from the sectional view in Figure 3, however, the punching cone is already completely formed. Considering the strong oscillations in the load time sequence, an increase of the average load to the mentioned capacity 0.86 MN expectedly would not be tolerable, because the remaining dowelling effect of the bending reinforcement presumably is not sufficient to prevent the entire perforation. This test result indicates that the load-bearing capacity of slabs without shear reinforcement is overestimated to a small extent by the formula given in DIN 25449, which has been developed mainly for slabs with shear reinforcement.

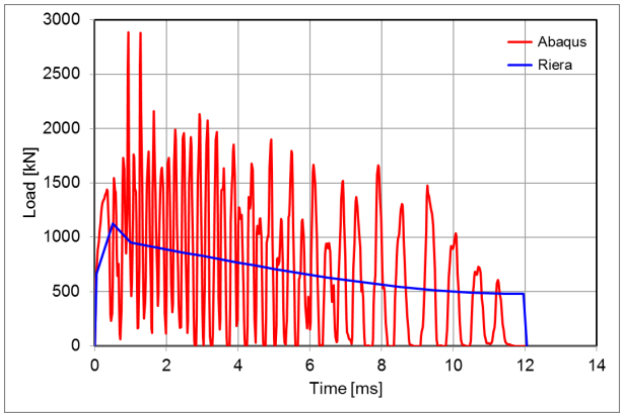

Figure 5: Test X5, load time functions for v = 162.5 m/s resulting from FE analysis with Abaqus and according to Riera approach.

NUMERICAL SIMULATION OF TESTS X6 TO X8

For the test slabs X6 to X8, the authors carried out numerical analyses using different three-dimensional (3D) FE models and different computer codes. The program SOFiSTiK (2014) was used by SPI, the program Abaqus, SIMULIA (2013), by Principia. The SOFiSTiK FE model is shown in Figure 6. The test slab is modelled by means of flat, multi-layered shell elements simulating the interaction of concrete and reinforcement. The arrangement of the bending and stirrup reinforcement in the centre of the test slab X6 is shown in Figure 7 together with the strain gauges on stirrups in the expected zone of the punching cone. The SOFiSTiK shell model cannot differ between various stirrup types, why the analysis results for test X6 are also valid for tests X7 and X8.

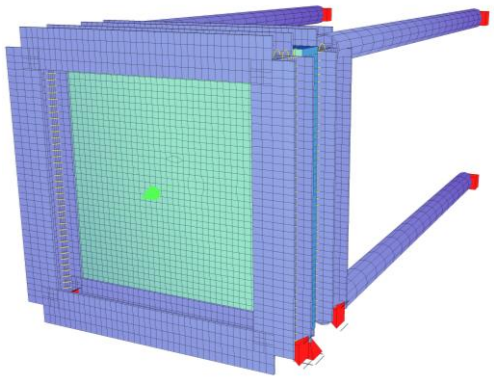

Figure 6. Tests X6 to X8, SOFiSTiK FE-model.

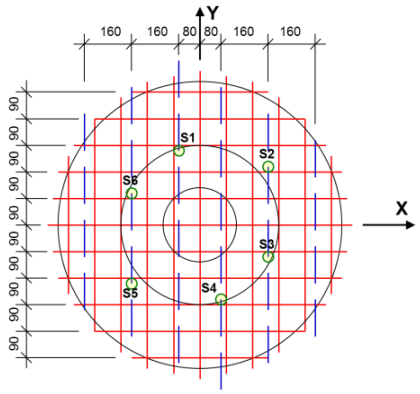

	Phase III Test X6	Phase III Test X7	Phase III Test X8
Transverse shear reinforcement	**Closed stirrups** 132 **Φ8mm** c/c 160mm / 180mm ⇨ **~ 34 cm²/m²**	**T-headed bars** 264 **Φ8mm** c/c 160mm / 90mm ⇨ **~ 34 cm²/m²**	**Hooked stirrups** 264 **Φ8mm** c/c 160mm / 90mm ⇨ **~ 34 cm²/m²**

Figure 7. Test X6, bending and shear reinforcement with locations of the gauges at the stirrups (equal in tests X7 and X8) and stirrup types.

The non-linear behaviour of the shear reinforcement in the SOFiSTiK analyses is simplified by means of an ideal-plastic shear stress / shear strain law. In order to determine the transverse force resistance in the punching zone, the shear reinforcement ratio and also the angle of the punching cone must be specified. The relevant punching cone angle was determined by evaluation of the intersection photos of a quarter of the test slabs X6 to X8 shown in Figure 8. An average angle of 48° was used for the test recalculations.

Furthermore, calculations of the tests X6 and X7 with the program Abaqus were performed by Principia. The bending reinforcement and the different shear reinforcement types are explicitly modelled as bar elements in the coupled FE model, see Figure 9. A distinction in the discretisation of T-headed bars and hooked stirrups could not be made in this FE model either.

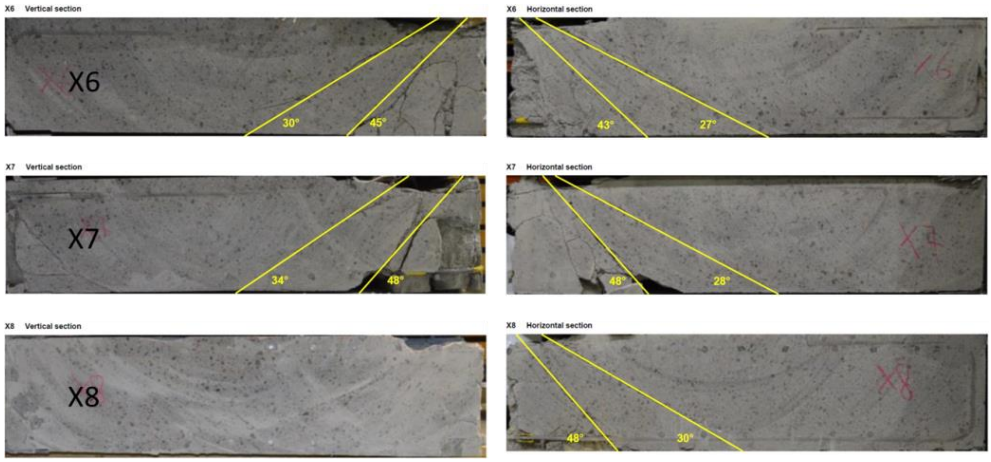

Figure 8. Tests X6 to X8, vertical (left) and horizontal intersections (right) with shear cracking.

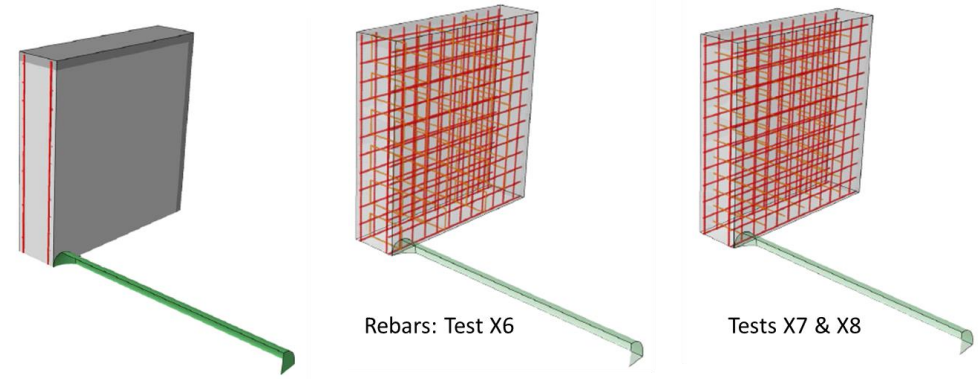

Figure 9. Tests X6 to X8, Abaqus FE model with arrangement of the reinforcement.

In the coupled Abaqus FE model, the applied forces results directly from the contact forces between the projectile and the slab. The diagram of Figure 10 shows a load time function derived from an Abaqus calculation for the impact on a rigid body. This load time function is used in the SOFiSTiK FE analysis.

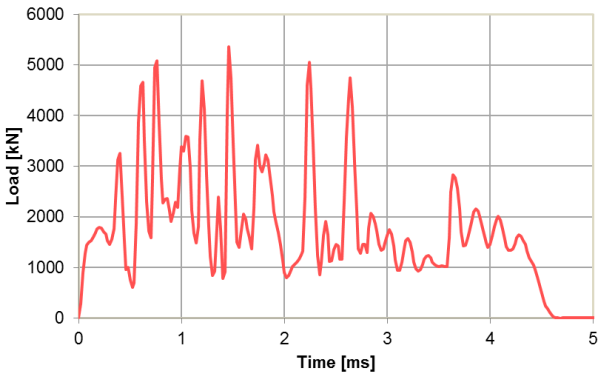

Figure 10. Tests X6 to X8, load time function for v = 167 m/s.

The calculation results in Figures 11 to 16 show time histories of displacements as well as steel strains of bending and shear reinforcement compared to the measured values. The computational simulation of the test results with the two different FE models has different degrees of accuracy. The displacements shown

in Figure 11 are overestimated in the punching zone by the Abaqus model and underestimated by the SOFiSTiK model. Outside the punching area, only slight deviations occur. Figure 12 shows that the strains in the bending reinforcement are reproduced by the SOFiSTiK analysis with appropriate accuracy.

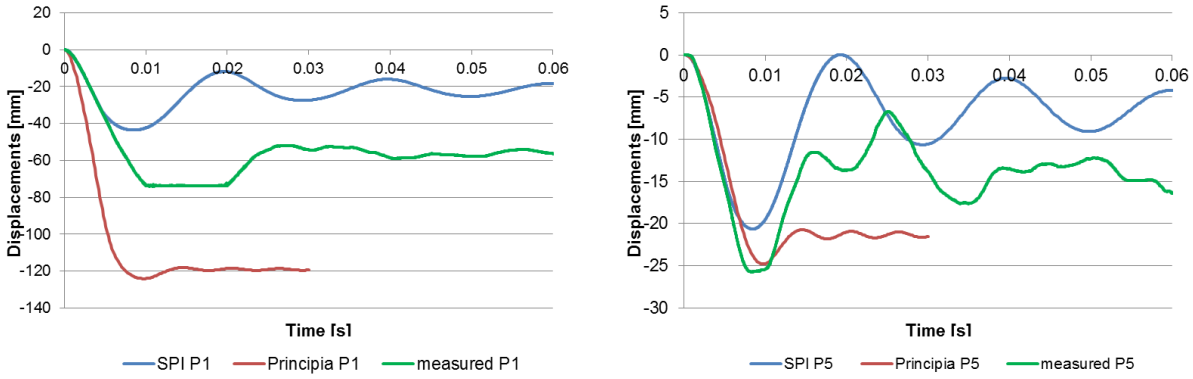

Figure 11. Test X6, calculated and measured displacements at the slab center (P1) and 540 mm aside (P5).

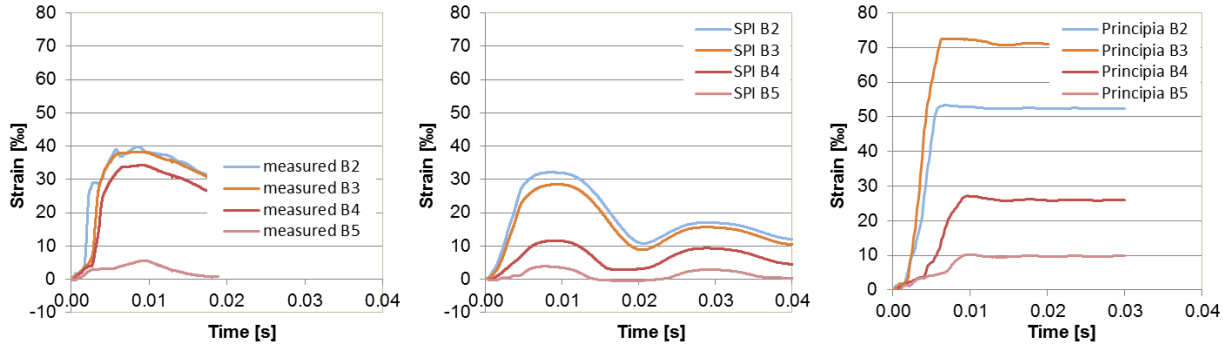

Figure 12. Test X6, calculated and measured strains of bending reinforcement in the vertical symmetry axis (B2 slab center, B3 to B5 at intervals of 135 mm below).

Strains of the shear reinforcement are evaluated in the Figures 13 to 15 for the three different shear reinforcement types. There are large deviations between calculated and measured values in almost all FE analyses, showing large fluctuations both on the measurement values and in the calculation results.

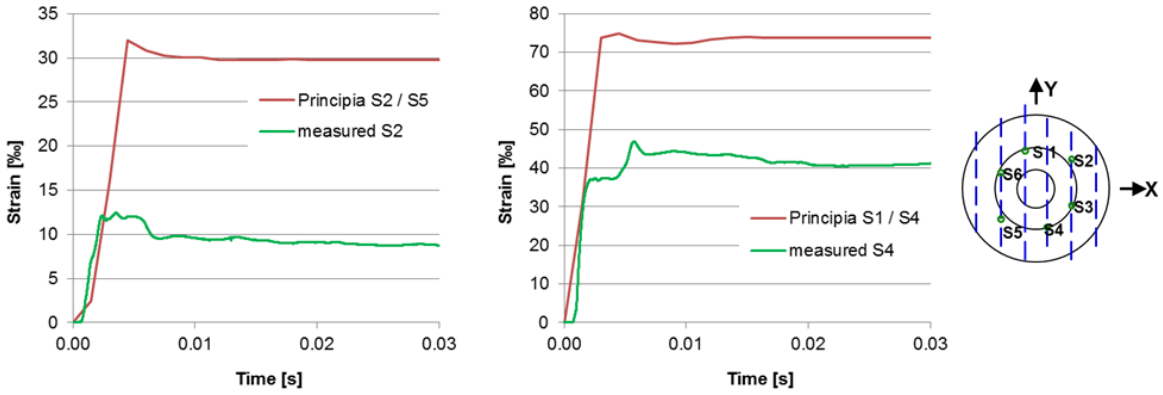

Figure 13. Test X6 (closed stirrups), calculated and measured strains of shear reinforcement for different positions.

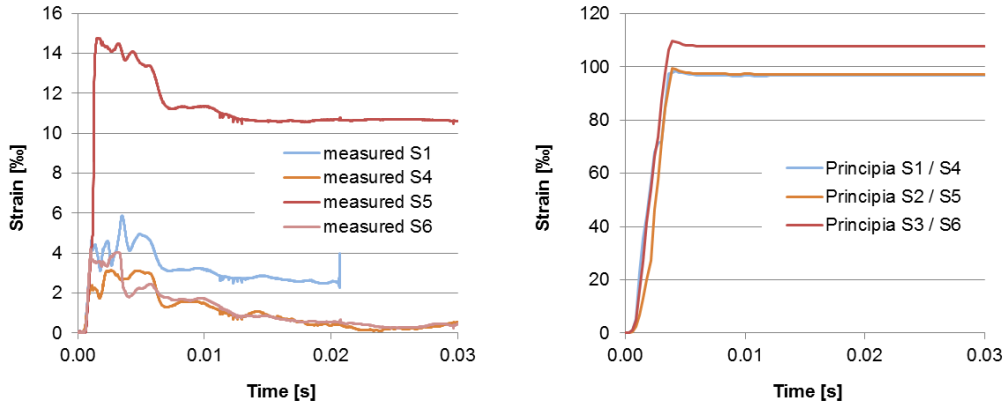

Figure 14. Test X7 (T-headed bars), calculated and measured strains of shear reinforcement for different positions.

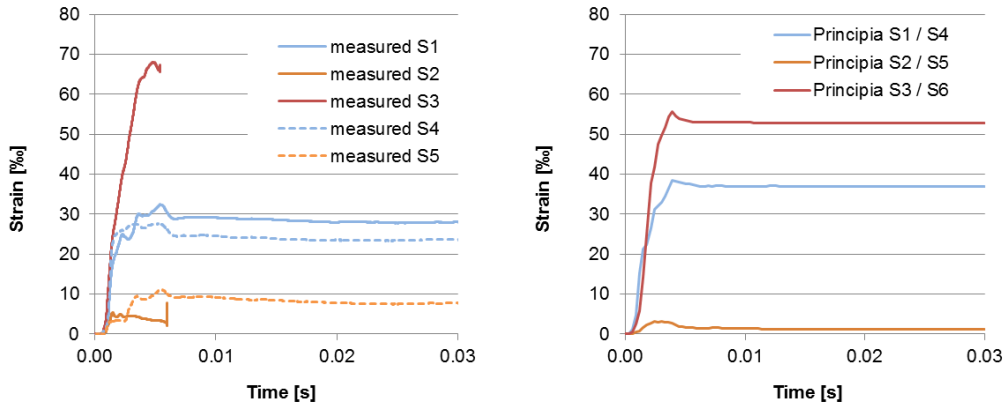

Figure 15. Test X8 (hooked stirrups), calculated and measured strains of shear reinforcement for different positions.

The observed differences in the measured values cannot be explained completely by the different reinforcement forms. They are also due to the local inhomogeneity of the r/c structure. The small deviations of the reinforcement positions from the slab symmetry as well as the slight differences between the concrete strengths of the individual experiments also in the numerical analyses produce comparatively large differences regarding the plastic deformations of the shear reinforcement. These findings lead to the conclusion that the numerical simulation of the combined bending and punching behaviour allows reliable statements about the integral ultimate capacity. But the strains of the shear transmission elements embedded in the concrete matrix in the punching area can hardly be reproduced in detail.

For the purpose of assessing the influence of the different shear reinforcement types, the displacements measured in the three tests in the centre of the slab and in two other equidistant positions aside are plotted over time in Figure 16. The measured data in test X6 (solid lines) are obviously erroneous, since the measured values are significantly larger than the permanent deformations recorded after the test, which are nearly identical in all three tests, cf. also Figure 1. The time histories of tests X7 and X8 in contrast are largely congruent and therefore to be considered plausible. Tests X6 to X8 thus suggest that the forms of shear reinforcement used did not have a significant effect on the punching behaviour of the test slabs.

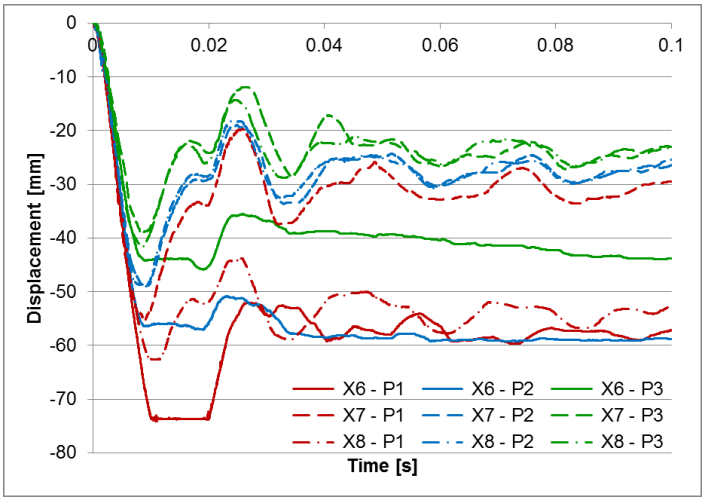

Figure 16. Tests X6 to X8, Comparison of measured displacements in the slab centre (P1), and 135 mm (P2) as well as 270 mm (P3) aside.

NUMERICAL SIMULATION OF TESTS X9 AND X10

The effect of different bending reinforcement ratios on the interaction of bending and punching behaviour is investigated in the tests X9 and X10. Test X8 serves as reference test for these experiments. Compared to the bending reinforcement of 8.7 cm^2/m in test X8, the reinforcement area is reduced to 5.6 cm^2/m (64%) in test X9 and increased to 12.6 cm^2/m (145%) in test X10. The other parameters of the tests widely coincide with those of test X8, see Table 1. Particularly, the reinforcement spacing could be maintained by sole change of the bar diameter.

Blind pre-calculations of tests X9 and X10 have been carried out by SPI with the SOFiSTiK FE model already used for the analysis of test X8, see Figure 6. The Abaqus load time function for an impact velocity of 167 m/s shown in Figure 10 has been used, too. In the Figures 17 and 18, calculated displacements and strains of the bending reinforcement of tests X8, X9 and X10 are compared to the measured results. The computed residual displacements fairly closely differ from the values of test X8 by a factor of 1.5 higher (X9) and lower (X10). Concerning the plastic strains of the bending reinforcement, this factor is 2.0.

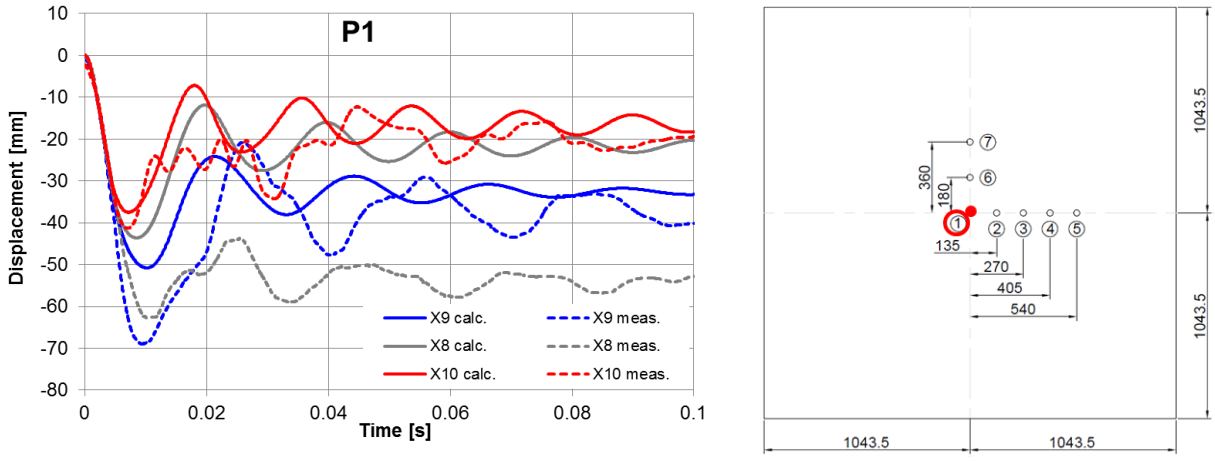

Figure 17. Tests X8, X9, X10, calculated and measured displacements for the centre of the slab.

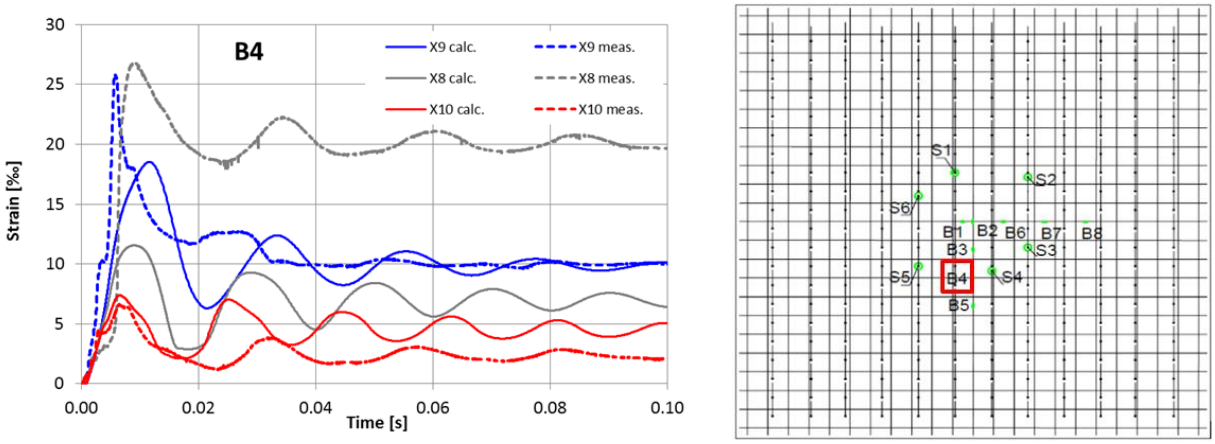

Figure 18. Tests X8, X9, X10, calculated and measured strains of bending reinforcement.

The maximum values of the measured displacements are larger than those of the calculated displacements, whereas the residual displacements are in good agreement. The deviations increase with decreasing bending reinforcement ratio presumably due to larger punching shear deformations, which are caused by steeper punching cone angles. In our calculations, an equal punching cone angle of 48° has been assumed for all three tests. The steel strains of the bending reinforcement show a comparably good agreement of calculated and measured maximum and residual values.

CONCLUSION

The comparison of experimental results and accompanying numerical simulations on different aspects regarding combined bending and punching behaviour of r/c panels demonstrates that the utilised computational methods are fundamentally capable of predicting the nonlinear mechanical behaviour of such structural elements when impacted by a deformable missile. It is shown that the computational analysis of slabs without transverse reinforcement needs FE modelling by use of volume elements when attaining the ultimate punching capacity. Moreover, the capacity of slabs without shear reinforcement appears to be overestimated to a small extent by the relevant German code provisions. The investigations on the tests with different types of shear reinforcement lead to the conclusion that the numerical simulation allows reliable statements about the integral ultimate capacity. But the strains of the shear transmission elements embedded in the concrete matrix in the punching area can hardly be reproduced in detail. Finally, the tests with different bending reinforcement ratios show that a decreasing bending reinforcement ratio under the same load leads to larger punching shear deformations.

REFERENCES

Borgerhoff, M., Schneeberger, C., Stangenberg, F., Zinn, R. (2013). "Conclusions from Combined Bending and Punching Tests for Aircraft Impact Design", Transactions, *SMiRT-22*, Division V, Paper no. 167, San Francisco, California.

Borgerhoff, M., Rodriguez, J., Schneeberger, C., Stangenberg, F., Zinn, R. (2015). "Knowledge from Further IMPACT III Tests of Reinforced Concrete Slabs in Combined Bending and Punching", Transactions, *SMiRT-23*, Division V, Paper no. 771, Manchester, United Kingdom.

SIMULIA (2013). "*Abaqus Analysis User's Manual*", Version 6.13, Rhode Island.

SOFiSTiK AG (2014). "*SOFiSTiK, Analysis Programs*", Version 30, Oberschleissheim.

Zinn, R., Borgerhoff, M., Stangenberg, F., Schneeberger, C., Rodríguez, J., Lacoma, L., Martínez, F., Martí, J. (2014). "Analysis of Combined Bending and Punching Tests of Reinforced Concrete Slabs within IMPACT III Project", *Eurodyn 2014, IX International Conference on Structural Dynamics*, Porto (Portugal).